Figure 2.9(a) Partially Dismantled Paste/Mortar Mould

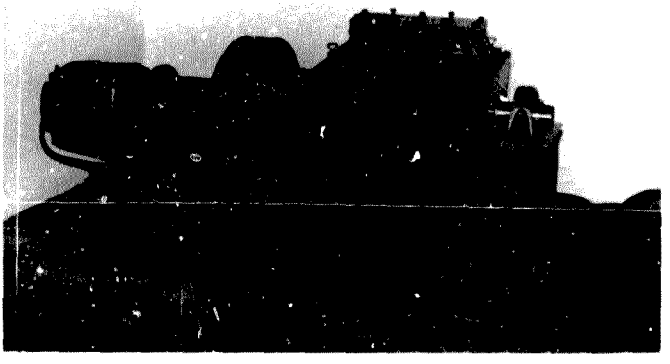

Figure 2.9(b) Moulds on Rotating Machine

was much less variation of effective cement/water ratio in the rotated specimen. Also he estimated that at 28 days the strength difference between the two specimens would be 8% and that within the non-rotated specimen there would be a 25% variation in strength from top to bottom due to segregation.

2.4.2 Mixing, Moulding and Curing Procedures for Pastes

Ordinary Portland cement, complying to SABS 471 (1982)[26], was used for all the pastes, mortars and concretes in this investigation. The cement was received fresh from the manufacturer in one batch. Each pocket of cement was then stored in an air tight drum in the laboratory. This batch of cement was used for all the tests carried out in this investigation.

The pastes were batched by mass allowing for a 20% wastage factor. An example of the mix design is given below for a cement/water ratio of 2,1.

Volume of paste $V_p = 4 \times 40 \times 40 \times 160 \times 10^{-9} = 1{,}024 \times 10^{-3}\ m^3$

Allow 20% wastage, $V_p = 1{,}2 \times 1{,}024 \times 10^{-3} = 1{,}229 \times 10^{-3}\ m^3$

For 1 litre of water, and cement/water ratio (c/w) = 2,1 :-

	mass (kg)		absolute volume (m^3)
water (R.D. = 1,00)	1	$\frac{1}{1000}$	$= 1{,}000 \times 10^{-3}$
cement (R.D. = 3,14)	2,1	$\frac{2{,}1}{3140}$	$= 6{,}688 \times 10^{-4}$
V' = absolute volume		V'	$= 1{,}669 \times 10^{-3} m^3$

Therefore for a mix of $V_p = 1{,}229.10^{-3} m^3$,

water required $= 1 \times \frac{1{,}229 \times 10^{-3}}{1{,}669 \times 10^{-3}} = 0{,}736$ kg

cement required $= 2{,}1 \times \frac{1{,}229 \times 10^{-3}}{1{,}669 \times 10^{-3}} = 1{,}546$ kg

Table 2.1 gives the paste mix proportions for the cement/water ratios used in the project. The cement and water were batched on a balance accurate to 0,1g. The water was slowly added to the cement during the first two minutes of mixing. The constituents were hand mixed for approximately 6 minutes. Great care was taken to eliminate unhydrated lumps of cement to ensure an even, smooth texture in the mix. The cement paste was poured into the mould up to about the 3/4 mark and the mould tamped on a table approximately 50 times to eliminate air bubbles entrained in the mould.

Table 2.1 Mix Proportions for Cement Paste Prisms

Cement/Water Ratio c/w	Mass of Cement g	Mass of Water g
2,4	1672	679
2,1	1546	736
1,8	1405	781
1,5	1067	889

These air bubbles were removed from the top surface by a spatula, the mould topped up to the brim and the top plate quickly screwed in place. Only one mould was poured at a time to help eliminate bleeding in the mix. The mould was immediately transferred to the rotating machine and rotated to prevent segregation.

The remaining paste mixture was then remixed by hand for approximately two minutes to mix in water which had bled to the top of the mixture. This procedure was repeated until all the paste moulds were filled. It was found that all cement/water ratios were pourable and bleeding was more acute in the lower cement/water ratios. For mould preparation see Appendix D. As previously stated, due to the problem of void formation in the low c/w ratio prisms, it was found necessary to add a super-plasticizing admixture (Pro-Struct 537) to the 1,5 cement/water

ratio mixes and this gave an acceptable specimen on demoulding. This admixture reduced bleeding by preventing flocculation. Alexander[27] also showed that this admixture had no effect on elastic modulus of concrete, therefore the elastic modulus results would not be adversely affected.

The pastes were demoulded with great care and stored in a water curing tank kept at 22°C ± 1°C. Despite all precautions, some specimens on demoulding or after failure contained sizeable voids either externally or internally within the specimen. Thus the result elastic modulus value would be affected by these voids and hence it often took several separate casting operations, especially for the lower c/w ratios, to achieve sufficient void-free specimens. Another alternative tried was to take the sealed mould and vibrate it similar to the technique employed by Stock, Hannant and Williams[28], but this was found to be an unsatisfactory solution. The reason for the voids was thought to be pockets of water which bled out of the mix and then evaporated, leaving macrovoids in the cement paste prism.

2.4.3 Mortar Mixes

Prismatic specimens with cement/water ratios of 2.4, 1.8 and 1.5 were cast. All specimens were tested in a saturated state at 28 days. Four prism specimens were cast in the moulds used for the pastes for each cement/water ratio and each aggregate sand type.

2.4.4 Mixing, Moulding and Curing Procedures for Mortar Mixes

The mix proportions for the mortars were extracted from the concrete mix designs and are tabulated in table 2.2(a) and 2.2(b) for granite and andesite mortars respectively.

The mortars were batched by mass, such that the absolute volume of mortar for the two different aggregate types was identical. The fractions for the mortar were extracted from the various concrete mix designs (see Chapter 3).

All the constituents were weigh batched on a balance accurate to 0,1g. The cement was added to the sand and thoroughly mixed for approximately two minutes to ensure uniformity. As with the pastes the mix water was added over the first two minutes of mixing. The constituents were hand mixed for an additional five minutes. The mortar was then poured into a steel mould. The mould was filled completely with the mix and then vibrated for thirty seconds on a vibrating table. This ensured adequate compaction and de-aeration of the specimen. The mould was sealed as previously described and bolted onto the rotating apparatus. The remaining mortar was remixed by hand for approximately two minutes to reblend the water which had bled to the surface. The procedure was repeated for all specimens. The prisms were rotated for 15-18h before demoulding. After demoulding they were transferred to a water bath to cure for 28 days in identical conditions to the paste specimens.

The mortars were easier to mix, mould and demould than the pastes. The specimens were more robust and did not require repeated recasting due to voids as did the lower cement/water ratio pastes.

2.4.5 Electrodynamic Testing of Pastes and Mortars

Before testing, each specimen was surface dried and weighed on a balance accurate to 0,1g. Then the physical dimensions were measured a minimum of three times by means of a vernier scale and centre lines were measured and marked in pencil. After each of the dynamic tests the prisms were returned to the curing tank. The theory and application of the electrodynamic modulus determination is covered in Appendix E. Essentially it is a

non-destructive convenient method of measuring the stiffness of a specimen. The specimen is vibrated and its natural frequency determined and hence the dynamic modulus of elasticity, E_d, is calculated. Basically a test specimen, in this case a prism, is supported at its nodal point, so that it may undergo free-free vibration without significant restraint (ie for longitudinal vibration it is supported at the centre). The drives and pick-up are shown in figure 2.10. The specimen is forced to vibrate at various frequencies; the frequency of vibration that gives maximum amplitude indicates the fundamental frequency. E_d was calculated using the expression given in appendix E.

The laboratory procedure is covered briefly in the following section.

The cured specimens were removed from the curing tank after 28 days and their dimensions and mass measured accurately. The prisms were wrapped in plastic wrapping to prevent moisture loss. Individual prisms were mounted in the electrodynamic apparatus as shown in figure 2.10. The vibrator and stylus pick-up were positioned accurately and the frequency of the vibrator varied by means of the frequency generator. When a peak or maximum amplitude occurred on the oscilloscope, the frequency was read off the frequency generator. This peak indicated the natural frequency of the specimen under test. Each frequency tabulated was an average of three readings. The frequency was varied until the maximum peak appeared on the oscilloscope indicating the natural frequency. This was recorded, the frequency reduced to zero, and the procedure repeated to give three values of the natural frequency.

Subsequent to the electrodynamic modulus determination of the pastes and mortars, a frequency counter was introduced into the circuit to enable the operator to obtain a more accurate reading of the natural frequency. Therefore all the natural frequencies

Table 2.2(a) Mix Proportions for Granite Mortars

CEMENT/WATER RATIO	WATER g	CEMENT g	SAND g
1,5	385	576	1751
1,8	385	694	1650
2,4	385	924	1408

Table 2.2(b) Mix Proportions for Andesite Mortars

CEMENT/WATER RATIO	WATER g	CEMENT g	SAND g
1,5	385	576	1883
1,8	385	694	1775
2,4	385	924	1568

of concrete were measured using the frequency counter. The electrodynamic modulus results for the pastes and mortars must therefore be treated with caution due to the 'crude' measurement of the natural frequency. The measured frequency was 'crude' in the sense that the frequency generator could only be read to the nearest 0,5 kHz, whereas the frequency counter gave readings accurate to within 10 Hz. Since E_d is proportional to the frequency squared, this would result in an error with respect to the dynamic modulus estimate. However, the frequency generator was later calibrated against the frequency counter and the initial results factored accordingly.

The results of electrodynamic elastic modulus tests are given in appendix E for the hardened cement pastes and mortars.

2.4.6 Ultrasonic Testing of Pastes and Mortars

The theory and application of the ultrasonic modulus method is covered in Appendix F. This method is based on the fact that the velocity of sound, V, in a material is related to the elastic modulus, E, by the expression

$$V = \sqrt{\frac{E}{\rho}} \qquad \ldots\ldots (2.2)$$

where ρ is the density of the material. Since the pulse velocity depends only on the elastic properties of the material and not on the geometry, this is a very convenient method to assess the ultrasonic dynamic elastic modulus. The apparatus is shown in figure 2.11 and is used to determine the pulse velocity through the known length of the specimen. In fact, mechanical impulses applied to a material generate three types of waves: longitudinal (compressional) waves, shear (transverse) waves and surface (Rayleigh) waves. The longitudinal waves are the fastest and are the waves that were transmitted in this particular

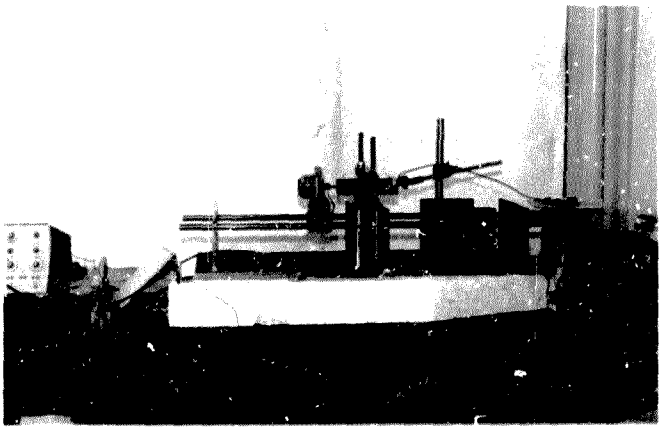

Figure 2.10 Paste Specimen Mounted in Electrodynamic Apparatus

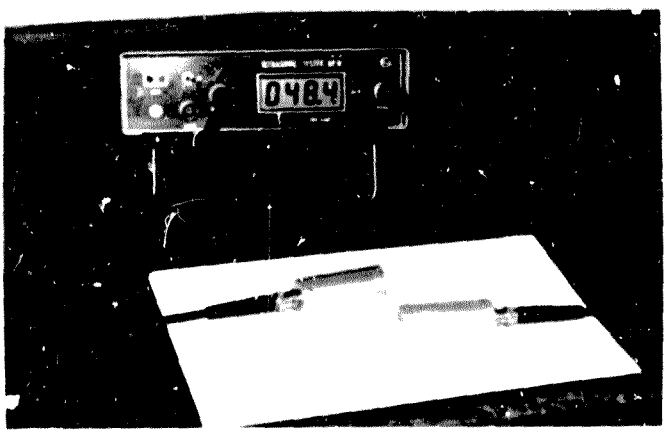

Figure 2.11 Ultrasonic Testing Apparatus

application. It should be noted that the ultrasonic equipment used for the pastes, mortars and concretes was different to that used in Chapter 1 for the rock cores. Petroleum jelly was used as a coupling agent between the prism and the ultrasonic heads. The prisms were surface dried with a cloth, the pulsing heads firmly applied at each ends of the specimen and the ultrasonic travel time recorded. Three measurements were recorded for one prism. The results for the ultrasonic dynamic elastic modulus tests are given in Appendix F for hardened cement pastes and mortars.

2.4.7 Static Modulus Test of Pastes and Mortars

The prisms were marked with centre lines and the gauge length of the static rig marked out. The static rig is fully described in Appendix D. This facilitated the fixing of the rig to the specimen and ensured that the extension of the prism under test was over the specified gauge length of 80mm. The rig was first fixed in the longitudinal direction, the locating screws both locating on the specimen at predetermined centre line pencil marks. This ensured an accurate gauge length for the test. The LVDT (linear variable differential transformer) and the adjustable screw were then lined up by adjusting the side locating screws (the longitudinal gauge length now being fixed). The lateral rig was positioned on the intersection of the longitudinal and lateral prism centre lines. Figure 2.12 shows a paste specimen held in the static paste/mortar rig. The prism was mounted in a Tinius Olsen machine and connected up to an X-Y recorder as described in Appendix C.

A preload of 0,5 MPa was applied to the specimen and held constant for approximately one minute. During this time the longitudinal and lateral LVDT's were zeroed by means of the adjusting screws and a multimeter. Thereafter, the pens recording the longitudinal and lateral extensions were also

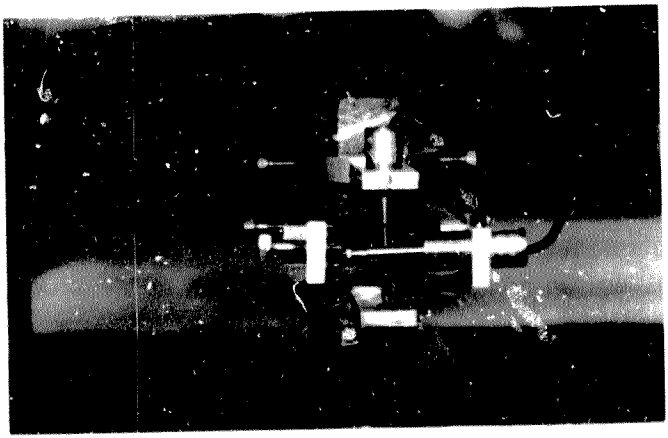

Figure 2.12 Paste Specimen Held in Static Test Rig

centred at a convenient origin, usually the top left hand corner of the X-Y chart. The load was applied at a constant rate of 24 kN/min (ie 15 MPa/min) up to $f_c/3$, where f_c was the 28 day compressive strength of the paste/mortar as given in Appendix C. (See also additional note on p 91(a)). For each cement/water ratio the 28 day strength was ascertained from a cement/water ratio against cube strength graph[29]. One third of this strength was calculated and a corresponding elastic modulus test limit load or 'E' load was calculated. Table 2.3 shows the 'E' loads ie one third of the expected failure load for pastes and mortars.

Once the 'E' load was reached, this load was held constant for one minute. The load was then removed at a rate of 24 kN/min and held at the pre-load for one minute. The X-Y recorder pens were re-zeroed and the specimen again loaded up to the 'E' load and unloaded, as described, to produce two more cycles. The elastic modulus of the specimen was determined from the third plot. Finally, the pens were re-zeroed and the specimen loaded at 24 kN/min up to failure, while the machine and X-Y recorder settings were altered accordingly. The results of the static elastic modulus tests are given in table 2.4 for pastes and tables 2.5(a) and 2.5(b) for granite and andesite mortars respectively. The final column of the tables indicates the failure mode of the specimens which is discussed in paragraph 2.5.1

2.5 RESULTS

It was originally hoped that the most important results would be those derived from the static tests, in order to be used in the theoretical models to determine predicted elastic modulus values. These results will be discussed in detail in this section followed by comparison with ultrasonic and electrodynamic modulus values.

Note:- The expected failure stresses for pastes, mortars and concretes were taken from one curve for concrete in the absence of more exact information. The writer is aware that failure stresses for pastes and mortars would tend to be greater than for that of concrete. However, the use of $f_c/3$ for the current tests was considered a consistent approach.

Table 2.3 Elastic Modulus 'E' Loads and Expected Failure Loads for Paste and Mortar Prisms

C/W RATIO	'E' LOAD kN	EXPECTED FAILURE LOAD kN
1,5	14,9	44,8
1,8	19,5	58,0
2,1	23,5	70,5
2,4	27,7	83,0

Table 2.4 Static Elastic Modulus Results for Pastes

SPECIMEN	LOAD AT FAILURE kN	STRESS AT FAILURE MPa	E_c GPa	ν	FAILURE TYPE
c/w = 1,5 1	12,9	8,10	4,60	0,27	Failed due to Voids
2	12,0	7,53	3,78	0,14	Failed due to Voids B
3	16,9	10,61	5,48	0,20	Failed due to Voids D
4	13,9	8,72	4,34	0,16	A
c/w = 1,8 1	29,2	18,32	6,64	0,18	B
2	24,5	15,29	5,59	0,22	Failed due to Voids B
3	18,9	11,86	5,67	0,20	Failed due to Voids B
4	22,9	14,35	5,57	0,17	Failed due to Voids B
c/w = 2,1 1	56,3	35,04	13,37	0,22	B
2	42,8	27,44	12,18	0,23	B

Table 2.4 Static Elastic Modulus Results for Pastes (continued)/...

SPECIMEN	LOAD AT FAILURE kN	STRESS AT FAILURE MPa	E_c GPa	ν	FAILURE TYPE
3	51,7	32,11	13,05	0,26	B
4	54,0	33,76	13,15	0,27	B
5	56,3	35,10	13,30	0,22	B
c/w 2,4 l	63,6	39,70	15,21	0,50	B
2	55,6	34,54	13,90	0,26	B
3	49,5	30,92	14,77	0,33	Failed due to Voids
4	63,5	39,35	13,52	0,24	A
5	56,4	35,49	12,23	0,26	B

Table 2.5(a) Static Elastic Modulus Results for Granite Mortars

SPECIMEN	LOAD AT FAILURE kN	STRESS AT FAILURE MPa	E_c GPa	ν	FAILURE TYPE
c/w = 1,5 1	25,6	15,75	14,26	0,17	D
2	27,9	18,15	15,79	0,18	D
3	28,0	18,04	14,91	0,16	A
4	24,0	15,66	12,54	0,15	A
c/w = 1,8 1	27,0	17,43	16,29	0,17	B
2	54,0	34,77	25,31	0,21	A
3	38,2	24,80	18,70	0,23	A
4	42,8	27,71	20,25	0,24	A
c/w = 2,4 1	91,0	58,96	29,80	0,24	C
2	84,0	53,87	29,77	0,25	A
3	81,8	53,13	29,76	0,26	A & B
4	Failure at 30,0 kN grossly concave 'E' curve. Therefore result not viable.				

Table 2.5(b) Static Elastic Modulus Results for Andesite Mortars

SPECIMEN	LOAD AT FAILURE kN	STRESS AT FAILURE MPa	E_c GPa	ν	FAILURE TYPE
c/w = 1,5 1	50,2	33,47	25,02	0,26	B
2	44,0	28,60	27,76	0,26	C & B
3	45,0	29,45	26,76	0,29	D
4	46,9	30,66	18,88	0,20	B
c/w = 1,8 1	60,6	39,11	24,03	0,20	D
2	70,2	45,36	28,47	0,21	A
3	62,2	40,18	25,26	0,21	A
4	67,8	43,90	23,81	0,25	B & D
c/w = 2,4 1	77,5	50,44	25,75	0,21	C
2	76,4	49,21	29,78	0,24	D
3	81,8	53,47	27,46	0,28	B
4	77,8	50,71	26,80	0,23	B

2.5.1 Static Elastic Moduli for Pastes

As stated in section 2.1 the stress-longitudinal strain and stress-lateral strain curves for paste are curvilinear. Figures 2.13(a) to 2.13(b) show copies of the X-Y recorder plots for a paste specimen, cement/water ratio of 2,1. These plots are representative of the recorded paste plots and are successive cycles on one specimen. The axes have been converted to stress and strain by use of calibration factors. The plots are all curvilinear for longitudinal and lateral strains but not excessively so. The loading and unloading components of the cycle are also nonlinear. The initial curve is more nonlinear than the successive curves. This is probably due to initial damage and structural change in the cement paste, namely compaction or consolidation occurring within the specimen. The slope of the initial or virgin curve also yields a lower elastic modulus than that of the third curve from which the elastic modulus was estimated. It can be seen that the area enclosed by the hysteresis loop of the initial curve is much greater than that of the successive cycles. This would be expected since during the "bedding in" cycle damage would occur and energy would be dissipated to a greater extent than in successive cycles. Figures 2.14, 2.15 and 2.16 show representative curves for c/w = 1,5, c/w = 1,8 and c/w = 2,4 pastes respectively. The curves for the pastes show that cement pastes are brittle materials and failure was always sudden, accompanied by sound emission from failure cracks. However, it must also be mentioned that brittleness depends on the type of testing machine used. Testing machines may be classified as hard (very rigid machines) or soft (less rigid machines). With a hard machine, the machine head will not follow rapid deformations of the specimen; a soft machine would follow these deformations. The machine used in this investigation is neither completely hard nor completely soft, but would tend to being a soft machine. The curves also show that when the specimens were held at the constant 'E-load', the paste exhibited more creep in the longitudinal direction than in the transverse direction.

The static elastic modulus was determined by choosing a convenient point near the 'E-load' value and the X, Y1 and Y2 distances measured back to the true origin, see figure 2.14. The slope of the plots were extrapolated back to zero to compensate for 'bedding in' of the rig which was not representative of the stress-strain plot (see figure 2.14). This produced a small horizontal portion near the origin. Although the pastes showed curvilinear stress-strain relationships, the curvature was not as pronounced as in the mortar and concrete plots. Thus the pastes tended to be more 'linearly elastic' in behaviour than mortars and concretes of identical c/w ratio. Table 2.6 shows the average values of static elastic moduli, prism compressive strength and static Poisson's ratio for the various cement pastes.

Table 2.6 shows that the values for prism compressive strength and static elastic moduli for the cement/water ratio pastes, 1,5 and 1,8 seem to be unrepresentative of true material behaviour. The expected failure stress for cement/water ratios 1,5 and 1,8 was 28 MPa and 36,3 MPa respectively. This is a difference of -58,7% between measured and predicted results (see table 2.7). Therefore, two different types of material behaviour are being measured. Table 2.7 shows that there appears to be a basic difference between the results for the lower cement/water ratios of 1,5 and 1,8 and the higher cement/water ratios of 2,1 and 2,4.

The difference could be explained by the presence of macrovoids in the pastes and possibly microvoids in the paste structure. The macrovoids were very much in evidence in the lower cement/water ratios, as discussed in section 2.4.1. It was thought that it might be possible to correlate strength and static elastic modulus with electrodynamic moduli, which are often considered to be comparable to the initial tangent modulus, due to the low stresses imposed by the dynamic test. However, it was decided that it would be invalid to correlate high cement/water ratio values for strength and static elastic moduli

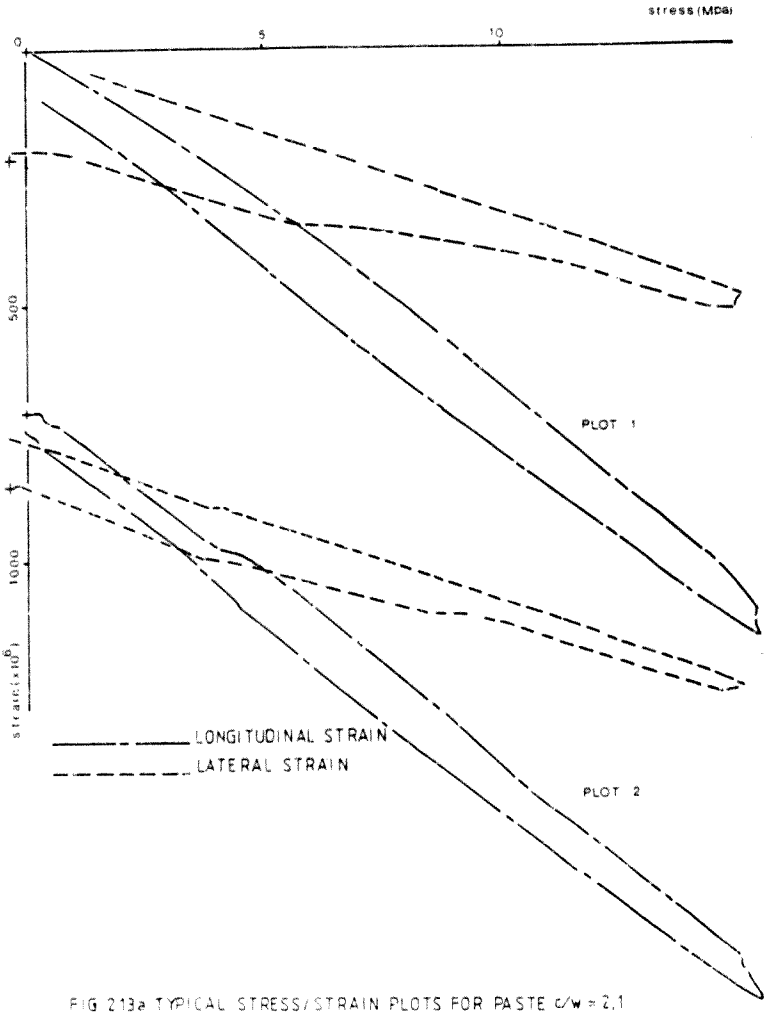

FIG 2.13a TYPICAL STRESS/STRAIN PLOTS FOR PASTE c/w = 2.1

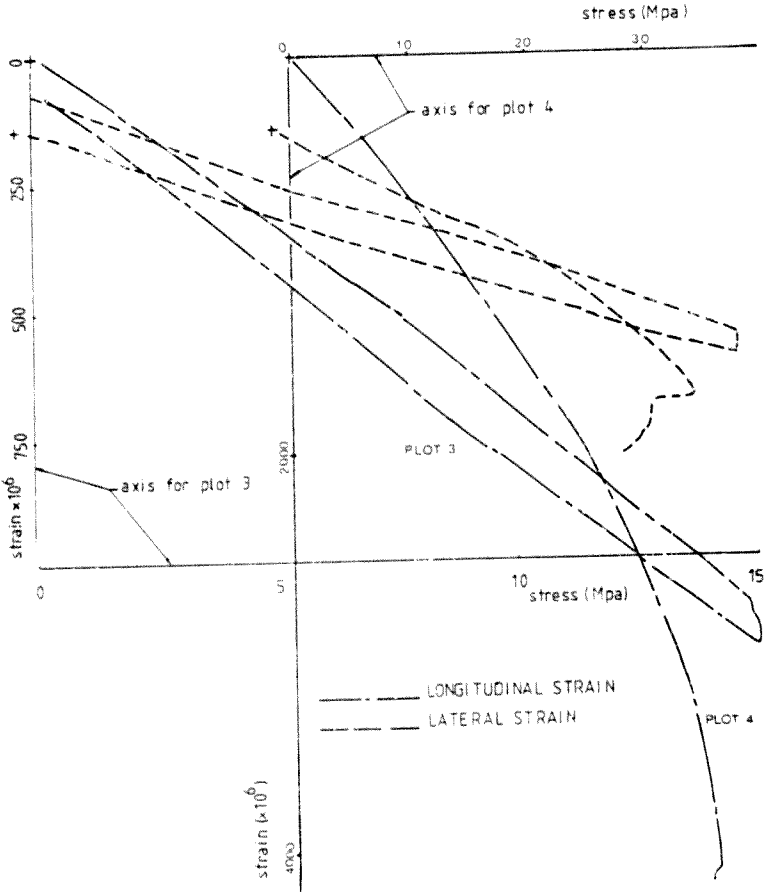

FIG 2.13b TYPICAL STRESS/STRAIN PLOTS FOR CEMENT PASTE c/w=2.1 PLOT 4 SHOWS COMPLETE STRESS/STRAIN CURVE

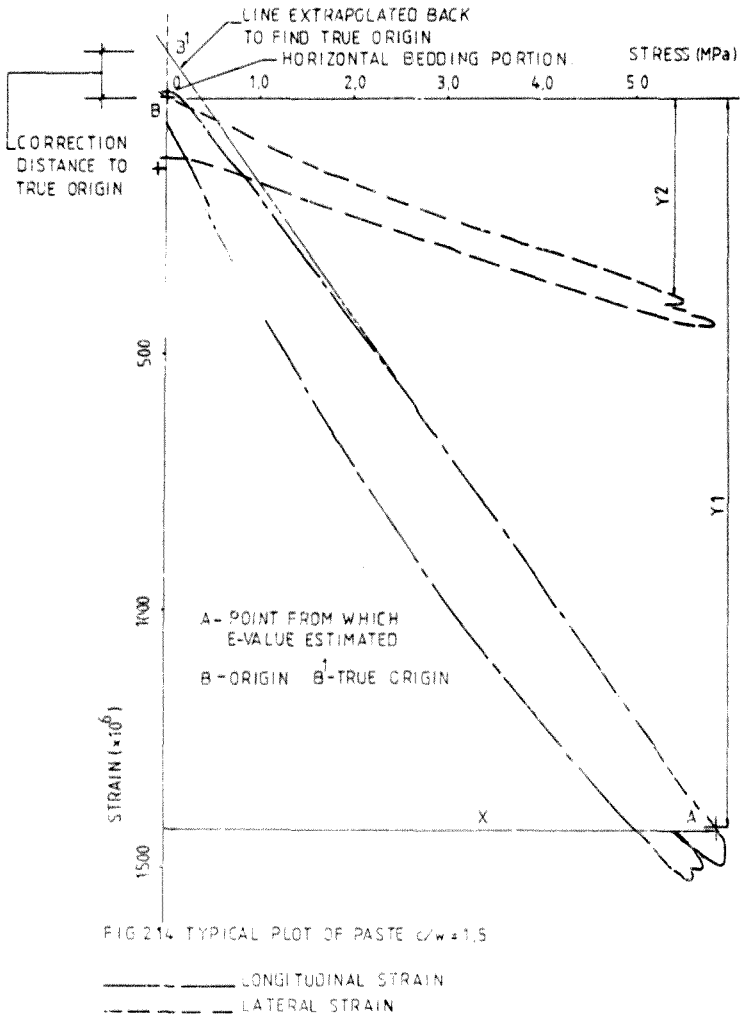

FIG 2.14 TYPICAL PLOT OF PASTE c/w = 1.5

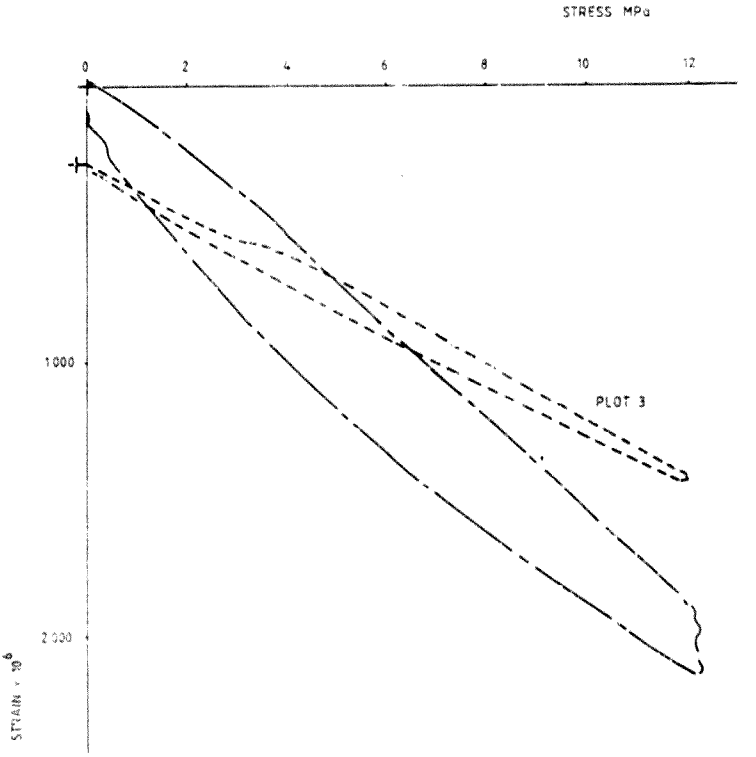

FIG 2.15 TYPICAL STRESS / STRAIN PLOT FOR PASTE c/w = 1.8

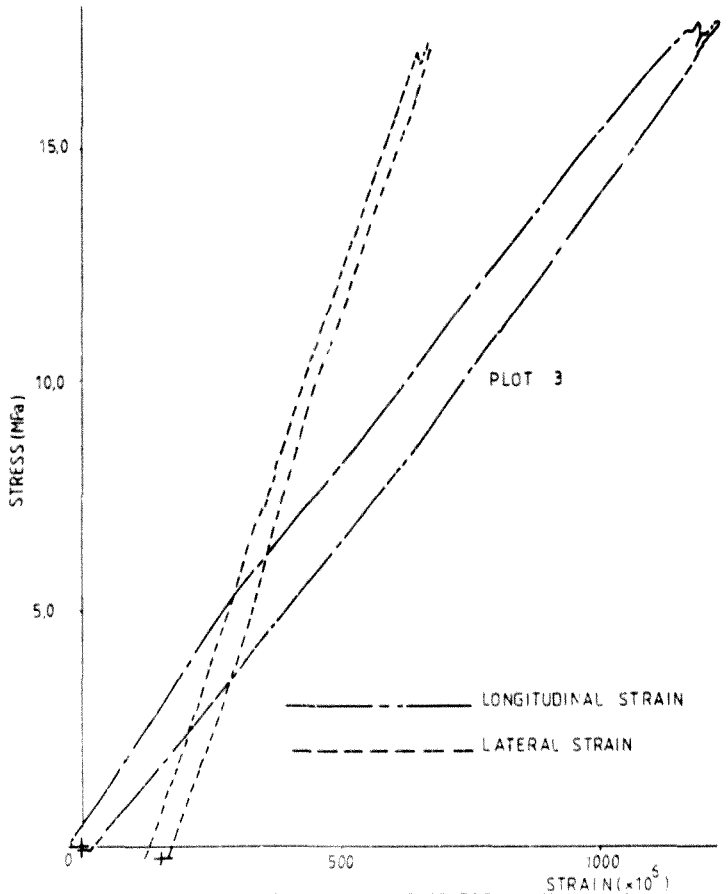

FIG 2.16 TYPICAL STRESS/STRAIN PLOT FOR PASTE c/w = 2.4

with electrodynamic modulus and then extend it to low cement/water ratios. Table 2.8 shows the average values of electrodynamic and ultrasonic modulus values for the pastes of the above cement/water ratios. The table confirms any correlation such as the one above would be invalid. The table shows slight variation of the electrodynamic modulus values of c/w values of 2,1 and 2,4. However the electrodynamic modulus varies quite considerably across the range of c/w ratios considered (ie c/w = 1,5 the electrodynamic modulus is 7,80 GPa and for a c/w ratio = 2,4 the modulus value is 17,28 GPa). Therefore any correlation may suggest only slight variation in the moduli for the lower c/w ratios. It can be seen from this table that there is only slight variation of the electrodynamic elastic modulus values for the range of cement/water ratios tested. Therefore, any correlation would be suspect. The writer is aware of this discrepancy with respect to these low cement/water ratios. Fortunately, only a small percentage of the investigation as a whole has been affected by the anomalies. The table shows that the ultrasonic dynamic modulus values are greater than the corresponding electrodynamic E values. Both vary in a similar way with c/w ratio.

Tables 2.4 and 2.5 indicate the various failure modes of the pastes and mortars. The failure types are shown diagramatically in figure 2.17(a). Three failed paste specimens are also shown in figure 2.17(b). Failure type A is a shear and tensile failure. Type B is a direct tensile failure and failure type D is a shear type failure caused by misalignment of the platen head of the loading machine giving rise to slight uneven load on the specimen. The curves used to predict failure loads were based on concrete cube strengths and would tend to be higher than that of a prism due to the aspect ratio effect.

2.5.2 Static Elastic Moduli for Mortars

Figures 2.18(a) and (b) and 2.19 and figures 2.20 to 2.21(a) and (b) show the X-Y recorder plots for the granite and andesite mortars

Table 2.6 Average Values of Static Elastic Modulus, Prism Compressive Strength and Poisson's Ratio for Cement Pastes

C/W RATIO	PRISM COMPRESSIVE STRENGTH MPa	STATIC ELASTIC MODULUS GPa	STATIC POISSON'S RATIO
1,5	13,93	4,55	0,19
1,8	14,96	5,87	0,19
2,1	32,69	13,01	0,24
2,4	36,00	13,93	0,28

Table 2.7 Prism Compressive Strength and Expected Failure Strength for Cement Pastes

C/W RATIO	PRISM COMPRESSIVE STRENGTH MPa	EXPECTED FAILURE STRESS (CUBE) MPa	% DIFF
1,5	13,93	28,00	-50,3
1,8	14,96	36,25	-58,7
2,1	32,96	44,06	-25,2
2,4	36,00	51,88	-30,6

$$\% \text{ Difference} = \left(\frac{\text{Measured} - \text{Predicted}}{\text{Predicted}}\right) \times 100$$

Table 2.8 Average Electrodynamic Elastic Modulus Values and Ultrasonic Elastic Modulus Values for Cement Pastes

C/W RATIO	ELECTRODYNAMIC MODULUS GPa	ULTRASONIC DYNAMIC MODULUS GPa
1,5	7,80	13,15
1,8	10,44	16,99
2,1	16,63	23,09
2,4	17,28	24,20

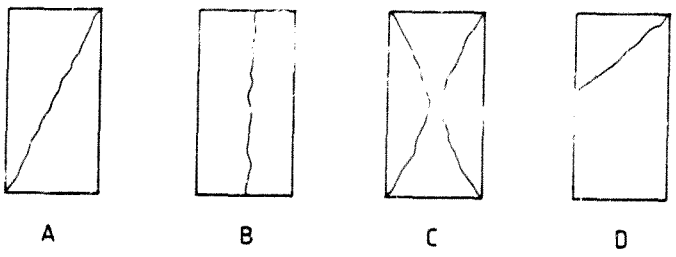

Figure 2.17(a) Prism Failure Types for Pastes and Mortars

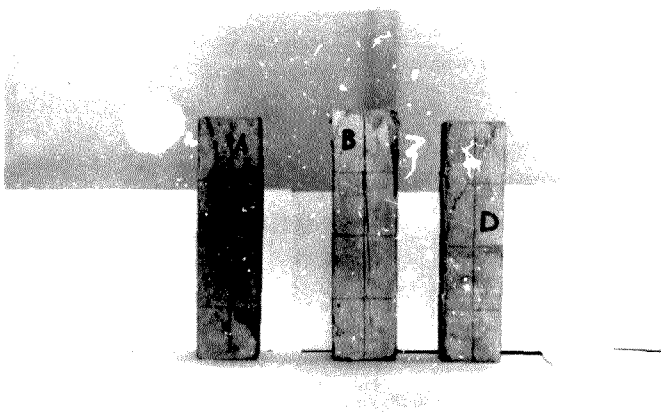

Figure 2.17(b) Failed Paste Specimens

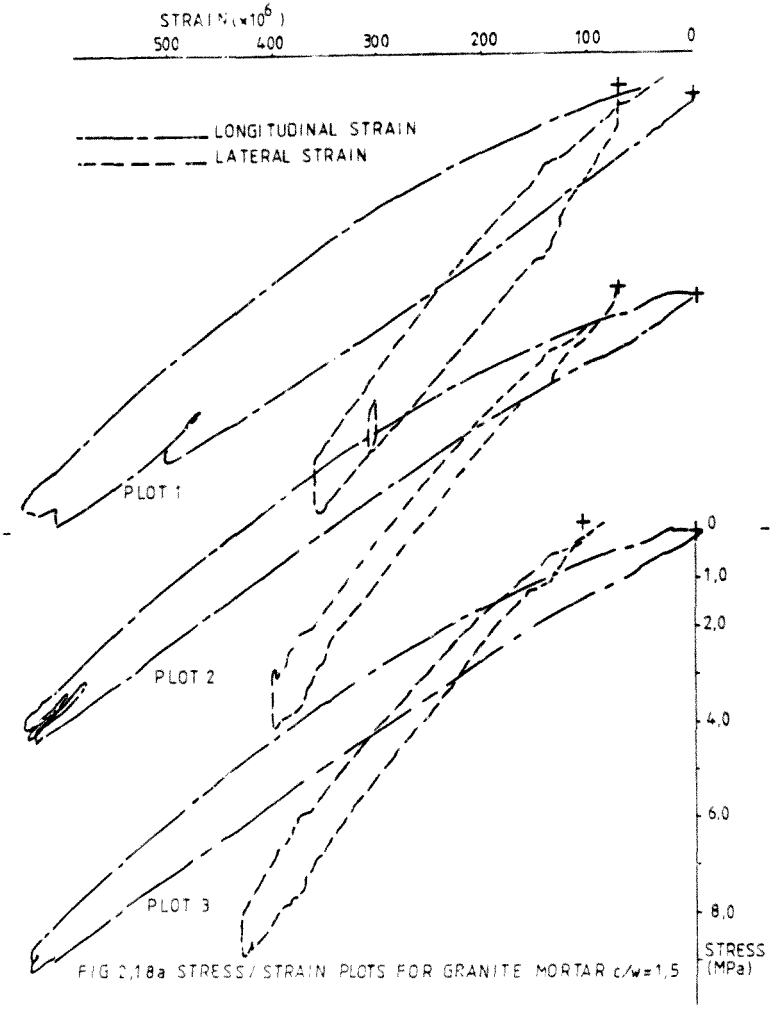

FIG 2,18a STRESS/STRAIN PLOTS FOR GRANITE MORTAR c/w=1,5

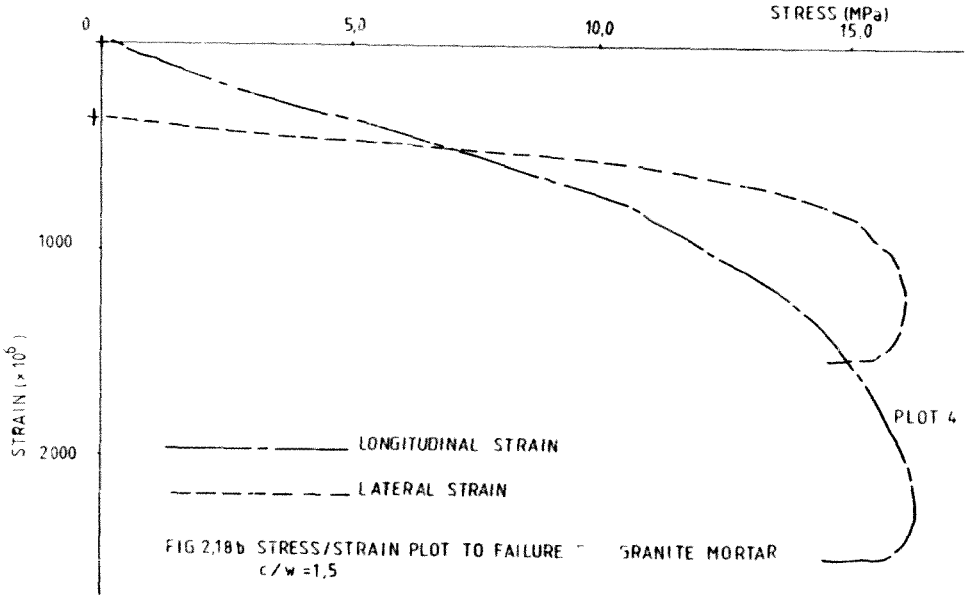

FIG 2,18b STRESS/STRAIN PLOT TO FAILURE - GRANITE MORTAR
c/w =1,5

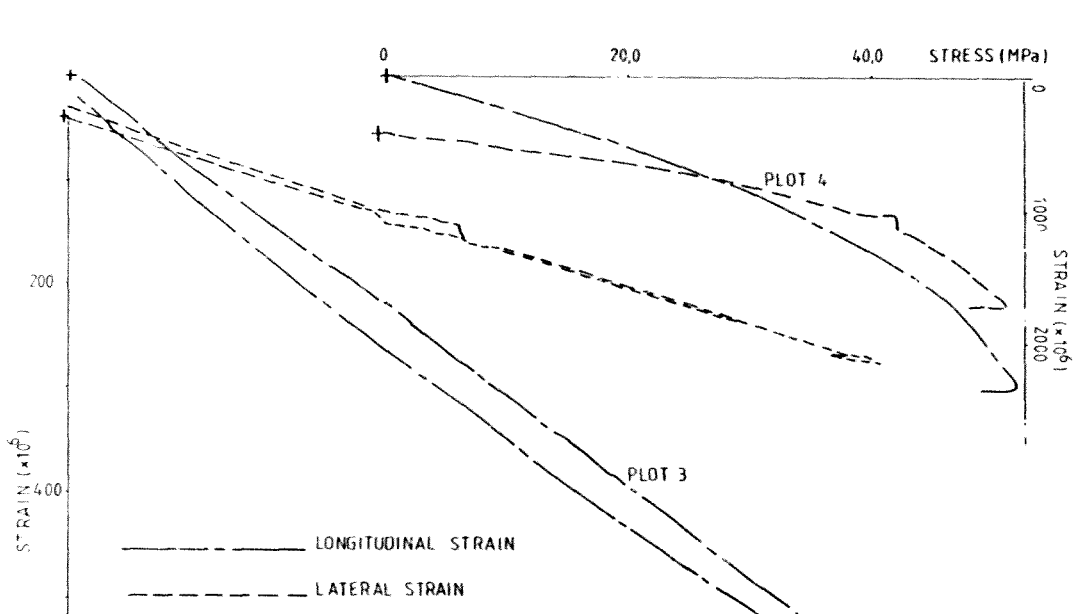

FIG 2.19 STRESS/STRAIN PLOTS FOR GRANITE MORTAR
c/w = 2,4

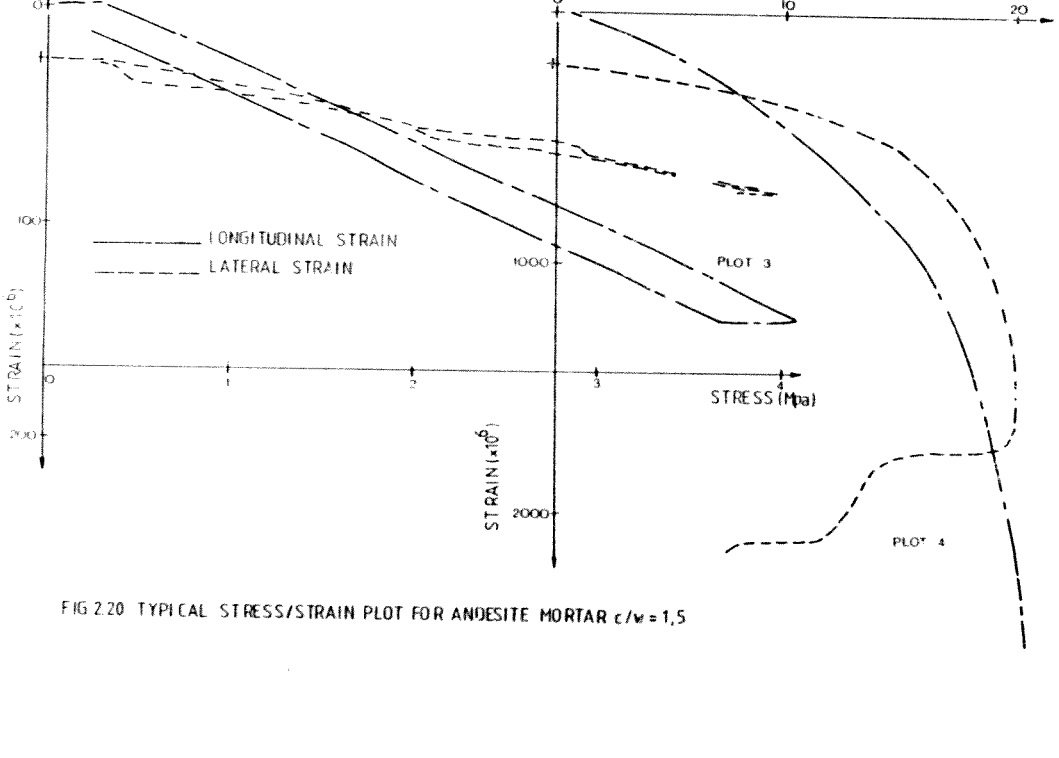

FIG 2.20 TYPICAL STRESS/STRAIN PLOT FOR ANDESITE MORTAR c/w = 1,5

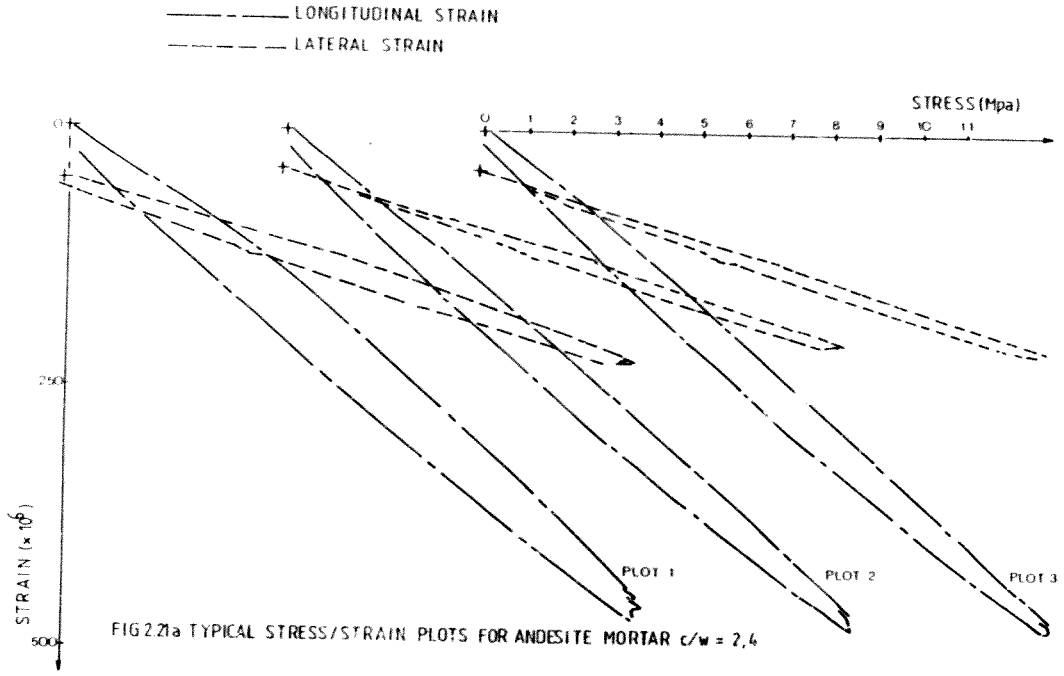

FIG 2.21a TYPICAL STRESS/STRAIN PLOTS FOR ANDESITE MORTAR c/w = 2,4

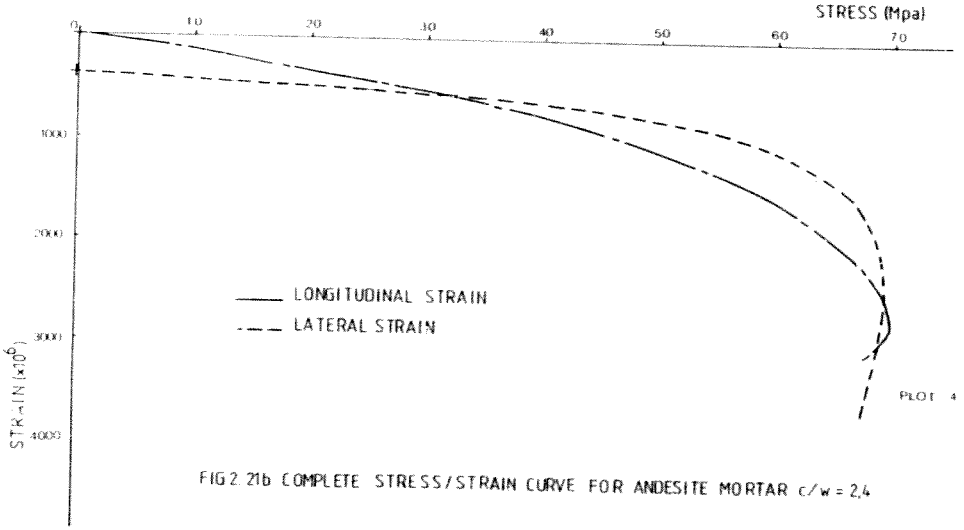

FIG 2.21b COMPLETE STRESS/STRAIN CURVE FOR ANDESITE MORTAR c/w = 2,4

respectively. Generally the mortars exhibit more curvilinear stress/strain plots than the pastes. An interesting observation is that the granite mortars, particularly for c/w ratio 1,5 and 1,8 exhibit stress/strain plots that are concave upwards. This suggests that the specimen is resisting deformation as load is applied and 'stiffening up' with increasing load. The longitudinal and lateral plots are both concave upwards for both loading and unloading cycles. This effect was only observed in the granite mortars. Table 2.9 shows that unrepresentative material behaviour is occurring in the granite mortars of cement/water ratios 1,5 and 1,8. This is evidenced by the low prism compressive strengths measured. The measured prism compressive strengths are well below the expected values as given in table 2.3. At the c/w ratios of 1,5 and 1,8 the comparative difference between the granite and respective andesite mortars is large, whereas at the c/w ratio of 2,4 the granite and andesite prism strengths are similar. The granite mortar gives both a higher strength and a higher elastic modulus than the andesite mortar for c/w = 2.4. Therefore, similar to the pastes there seems to be a basic difference between the granite mortar results for the lower c/w ratios and the high c/w ratios, especially with respect to strength. This effect is still apparent in the values for elastic modulus, but to a lesser extent. As discussed in section 2.5.1 this is thought to be due to the presence of micro voids in the granite mortars, so that a different material behaviour is being measured. It is possible at these low c/w ratios that the crushed granite sand was slightly deficient in fine material which leads to the presence of voids. The andesite crushed sand was more uniform than the granite sand and had relatively more fines in its composition. This is evident from the grading analysis given in Appendix A. Several of the granite mortar failure mechanisms at the lower c/w ratios were failure type 'D'. This is a shear type failure resulting in an apparently lower compressive strength. This could explain the observation of the concave-upward X-Y plots for both cement/water ratios 1,5 and 1,8 for the granites. Again the writer is aware of this discrepancy in the investigation, but it must be viewed as a small part of the whole investigation. Correlations with measured dynamic moduli were

inadvisable as discussed in section 2.5.1. The hysteresis effects mentioned in section 2.5.1 were also evident for the mortars and the initial 'bedding in' of the test rig was much more pronounced than for that of the pastes. The energy dissipated reduced with each load cycle, indicated by the reduced enclosed area between the loading and unloading curve.

The static elastic modulus was calculated in an identical manner to that of the pastes. Again the virgin curve for each mortar gave a lower elastic modulus than that of the final curve mainly due to compaction and consolidation of the specimens over successive loading cycles. The plots were show the mortar to be more 'ductile' than the pastes, given by the presence of a continuing plot after the maximum stress had been reached. The mortar failures were not as catastrophic as the pastes although the failure was still sudden. Tables 2.5(a) and 2.5(b) show that for each c/w ratio both granite and andesite mortars gave consistent results. Tables 2.9 and 2.10 give the average values of static elastic moduli, prism compressive strength and static Poisson's ratio for granite and andesite mortars respectively.

As expected the andesite mortars gave higher static elastic moduli than their granite counterparts with the exception of cement/water ratio 2,4. The elastic modulus of the andesite mortars seems to be only slightly affected by increase in cement/water ratio as opposed to the granites which exhibit a marked effect. The andesite prism failure stresses were also much higher than those of the respective pastes and failed at expected stresses as did the granite mortar specimens of cement/water ratio 2,4.

Tables 2.5(a) and 2.5(b) also show that no specimens failed due to macrovoids, therefore the strength estimates are more reliable than those of the pastes, with the exception of the granite mortar prisms of cement/water ratios 1,5 and 1,8. Some of the prisms exhibited failure type 'C' which was characteristic of many of the concretes tested. Figure 2.22 shows a plot of

Table 2.9 Average Values of Static Elastic Modulus, Prism Compressive Strength and Poisson's Ratio for Granite Mortars

C/W RATIO	PRISM COMPRESSIVE STRENGTH MPa	STATIC ELASTIC MODULUS GPa	STATIC POISSON'S RATIO
1,5	17,15	14,38	0,17
1,8	26,18	20,14	0,21
2,4	55,32	29,78	0,25

Table 2.10 Average Values of Static Elastic Modulus, Prism Compressive Strength and Poisson's Ratio for Andesite Mortars

C/W RATIO	PRISM COMPRESSIVE STRENGTH MPa	STATIC ELASTIC MODULUS GPa	STATIC POISSON'S RATIO
1,5	30,55	24,61	0,25
1,8	42,14	25,39	0,27
2,4	50,96	26,70	0,22

prism compressive strength against static modulus of elasticity for andesite mortars. The granites showed greater spread in both static modulus and prism strength values. Figure 2.22 shows that the static elastic modulus varied very little with compressive strength. One possible explanation for this is that the range of volume fractions of paste and sand over the range of mortars studies is fairly small. Also paste moduli are low relative to sand moduli, thus offsetting increase in mortar modulus with increase in strength which involves an increase in paste content here. This would endorse Davis[29] findings as mentioned in section 2.3, that rich mortars, because of their high paste content, had significantly lower moduli relative to their respective concretes. Conversely, lean mortars rendered relatively high elastic moduli.

2.5.3 Comparison of Elastic Moduli for Pastes and Mortars

The results for the electrodynamic and ultrasonic dynamic elastic moduli are given in tables 2.8, 2.11(a) and 2.11(b) for cement pastes, granite and andesite mortars respectively. The tables show that the ultrasonic modulus was the highest followed by electrodynamic and lastly static elastic moduli for pastes and mortars. Figure 2.23 shows that all three moduli follow roughly the same form when plotted against cment/water ratio for andesite mortar. The plot also demonstrates that the modulus of elasticity of all three moduli vary very little with increasing cement/water ratio.

The andesite mortars gave the highest ultrasonic and electrodynamic moduli followed by the granite mortars and finally the pastes. The dynamic tests also rendered the most consistent results, especially the ultrasonic tests. This may be attributed to the fact that the dynamic measurements are not as sensitive to inherent flaws in the specimens, as the specimens are subjected to negligible stress while under test. Figure 2.24 shows the plots of static elastic modulus against electrodynamic and

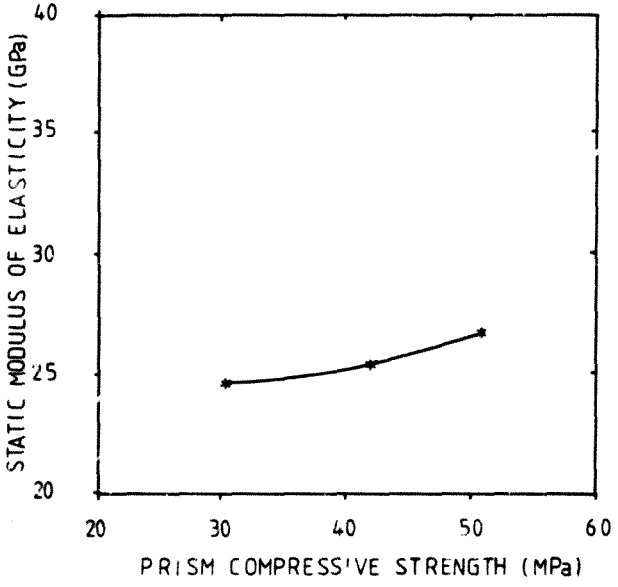

FIG 2.22 PRISM COMPRESSIVE STRENGTH Vs.
STATIC MODULUS (ANDESITE MORTARS)

SOLID LINE: STATIC MODULUS
DOTTED LINE: ELECTRODYNAMIC MODULUS
CHAIN LINE: ULTRASONIC MODULUS

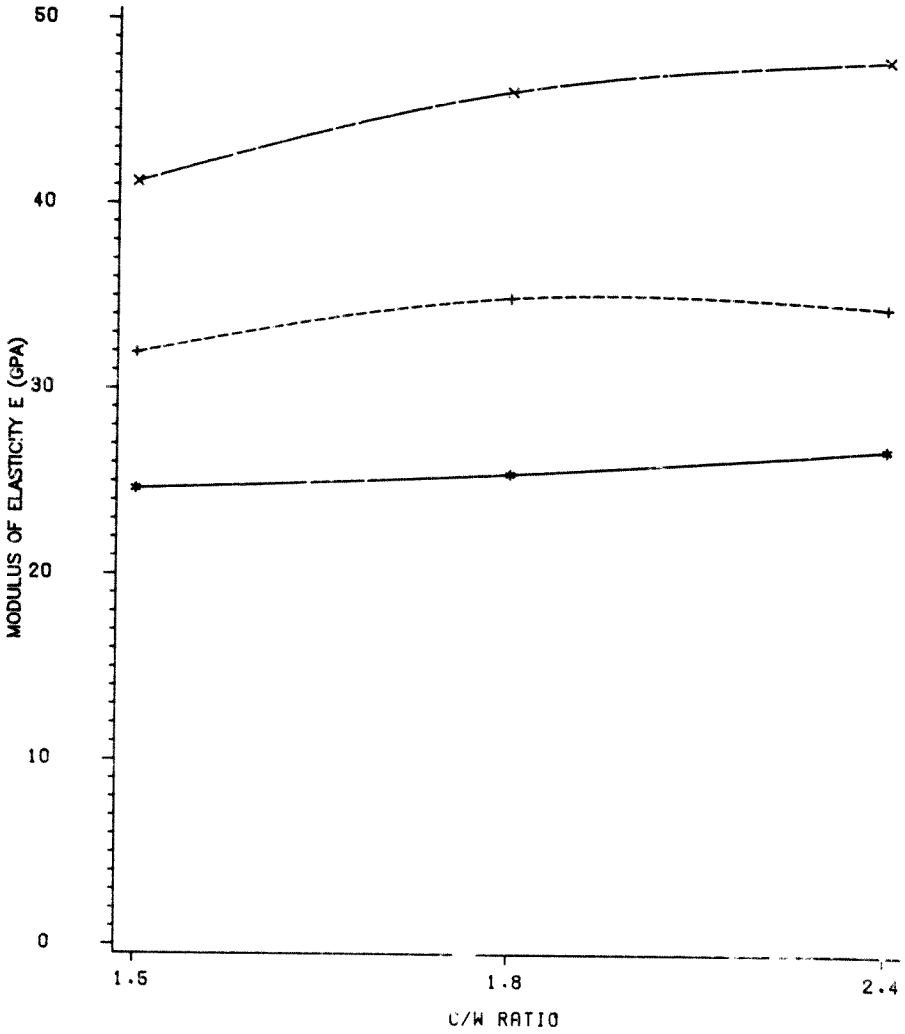

FIG 2.23 C/W RATIO VS. MODULUS OF ELASTICITY
ELASTIC MODULUS PLOTS FOR AN[illegible]TE MORTARS.

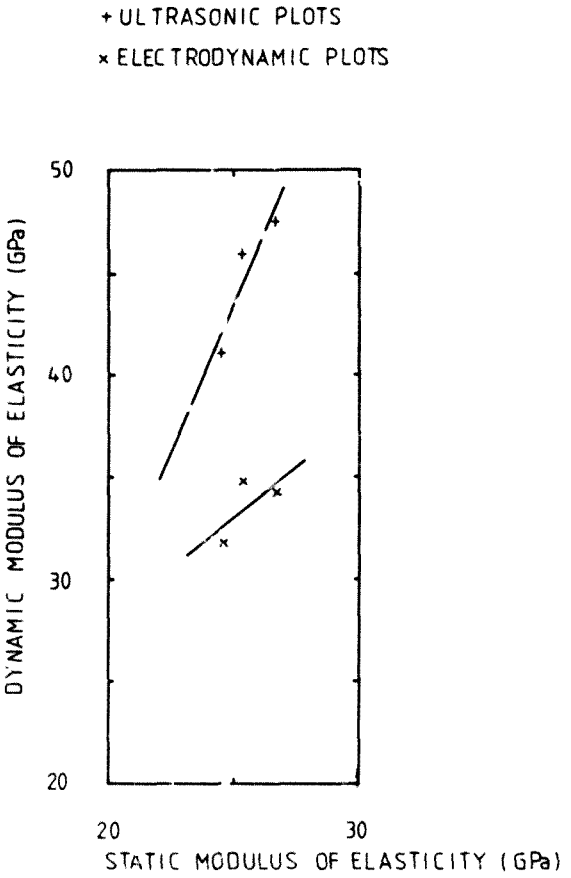

FIG 2.24 STATIC MODULUS Vs. ELECTRODYNAMIC AND ULTRASONIC DYNAMIC MODULUS FOR ANDESITE MORTARS

Table 2.11(a) Average Electrodynamic Elastic Modulus Values and Ultrasonic Elastic Modulus Values for Granite Mortars

C/W RATIO	ELECTRODYNAMIC MODULUS GPa	ULTRASONIC DYNAMIC MODULUS GPa
1,5	26,17	38,17
1,8	31,69	40,91
2,4	35,96	45,28

Table 2.11(b) Average Electrodynamic Elastic Modulus Values and Ultrasonic Elastic Modulus Values for Andesite Mortars

C/W RATIO	ELECTRODYNAMIC MODULUS GPa	ULTRASONIC DYNAMIC MODULUS GPa
1,5	31,93	41,17
1,8	34,88	46,01
2,4	34,34	47,63

Table 2.12 Average Static Elastic Modulus Values for Cement Pastes, Granite and Andesite Mortars

C/W RATIO	CEMENT PASTE GPa	GRANITE MORTAR GPa	ANDESITE MORTAR GPa
1,5	4,55*	14,38*	24,61
1,8	5,87*	20,14*	25,39
2,1	13,01	-	-
2,4	13,93	29,78	26,70

Values marked * are regarded as unrepresentative of true material behaviour as discussed in sections 2.5.1 and 2.5.2

ultrasonic dynamic moduli for andesite mortars. If a statistically significant number of tests were carried out, good correlation between dynamic and static moduli could be established, provided valid static results can be obtained.

The values given in table 2.12 for pastes, granite mortars and andesite mortars for each cement/water ratio tested are used in chapter 4 to predict values of the elastic modulus of concrete using the theoretical models. Values regarded as unrepresentative of true material behaviour are redundant in this respect.

2.6 CONCLUSIONS

1. Pastes are much more sensitive to casting technique than mortars. Care must be taken to ensure uniformity of the specimen. This is especially important at the lower c/w ratios, particularly 1,5.

2. The andesite mortars gave the highest strengths and the most consistent elastic modulus results. Due to different material behaviour at c/w ratios of 1,5 and 1,8 the results for the hardened cement pastes and granite mortars cannot be regarded as representative of "true" material behaviour.

3. For the range of c/w ratios tested, both the static and dynamic elastic moduli do not vary very much with increasing c/w ratio.

4. The dynamic testing was easier and quicker to carry out than the static testing. The results of the dynamic tests were also more consistent than the static tests.

5. The pastes gave reasonably linear-elastic stress/strain curves, and failed in an abrupt brittle fashion. However, the elastic modulus results were not as consistent as for the mortars. The stress/strain plots for mortars resembled that of the concretes. However, some of the granite mortar curves at the lower c/w ratios exhibited concave-upward stress/strain plots. This was felt to be unrepresentative material behaviour, endorsed by the low static elastic moduli and compressive strengths recorded for these specimens.